Transitions of flow between two corotating disks in an enclosure

Jiro Mizushima[1] and Tomohito Miura[1]

Summary

Transitions of flow between two corotating disks in an enclosure are investigated numerically and experimentally. The outer cylindrical boundary of the flow field is assumed being fixed, whereas the inner cylinder (hub) rotating together with the two disks. The flow is not only symmetric with respect to the inter-disk midplane but also axisymmetric around the axis of rotation at small Reynolds numbers although it becomes unstable to disturbances at high Reynolds numbers. Two kinds of instability modes are known, one of which is an axisymmetry-breaking instability mode to yield a polygonal flow pattern in the radial tangential plane which occurs for small gap ratios, the ratio of the gap between two disks to the radius of the annulus. The other is a symmetry-breaking instability mode with respect to the inter-disk midplane while retaining the axisymmetry, which occurs for moderate gap ratios. We focus our attention on the symmetry-breaking instabilty and assume the axisymmetry of the flow field. We obtain steady axisymmetric flows numerically and analyze their linear stability. It is found that the steady axisymmetric flow is unstable not only to stationary disturbances but also to oscillatory disturbances, which results in steady or oscillatory asymmetric flow, respectively. That is, the symmetry-breaking instability is classified into stationary and oscillatory symmetry-breaking instabilities. Numerical simulations are also performed to obtain time-periodic flows, and bifurcation diagrams of the flow are depicted for various values of gap ratio. The critical Reynolds numbers for the two symmetry-breaking instabilities are evaluated and a transition diagram is obtained. Our numerical results are confirmed by experiments.

Introduction

The flow between two corotating disks enclosed in a stationary outer casing has been investigated as a simple model of computer disk strages, and shown to exhibit a variety of flow patterns. This flow is also regarded as a short-length case of Taylor-Couette flow in a cylindrical annulus. The flow has two symmetries, one of which is the axisymmetry around the rotation axis and the other the reflectional symmetry with respect to the inter-disk midplane. At small Reynolds numbers, the flow is inter-disk symmetric as well as axisymmetric irrespective of the gap ratio, the ratio of the gap between the two disks to the radius of the annulus. However, at large Reynolds numbers it becomes unstable to time-dependent axisymmetry-breaking disturbances which results in an appearance of polygonal shape in the radial-tangential plane for small gap ratios. For moderate gap ratios, it becomes unstable to stationary or oscillatory symmetry-breaking disturbances yielding an asymmetric flow pattern with respect to the inter-disk midplane while retaining the axisymmetry.

Polygonal flow patterns in the radial-tangential plane were observed in experiments by Lenneman[1]. The objective in his experiments was a reduction of disk flutter in computer

[1]Department of Mechanical Engineering, Faculty of Engineering, Doshisha University, Kyotanabe, Kyoto610-0321, Japan

disk strages. The structure in the flow was investigated by using a flow visualization method by Abrahamson, Eaton and Koga[2].

An asymmetric flow with respect to the inter-disk midplane was found in experiments and numerical calculations by Tavener, Mullin and Cliffe[3], who revealed that the asymmetry arises due to an inter-disk symmetry-breaking (pitchfork) bifurcation from a symmetric flow. On the other hand, Herrero *et al.*[4] clarified that the polygonal flow patterns appear due to a Hopf bifurcation from the axisymmetric flow. A regime diagram of these bifurcations in a parameter space consisting of the Reynolds number and gap ratio was obtained by Randriamampianina *et al.*[5] and a critical gap ratio was determined where the pitchfork and Hopf bifurcations interchange.

Our objective in the present paper is to clarify the bifurcation structure of the flow between the two corotating disks and explore the underlying physics of the appearance of various flow patterns under the assumption of axisymmetric flow field for moderate gap ratios.

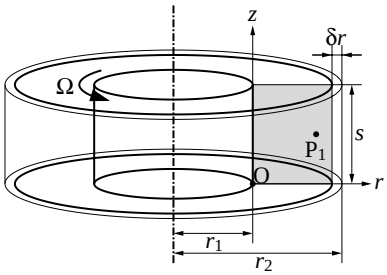

Figure 1: Configuration and coordinates.

Definition and formulation of the problem

We consider fluid motions between two corotaing disks in an enclosure, where the outer cylinder of radius r_2 is fixed and the inner cylinder (hub) of radius r_1 rotating together with the two disks with angular velocity Ω (Figure 1). The spacing δr between the edge of disks and the outer cylinder is neglected theoretically, but is finite in experiments. The gap between the two disks is s and the gap ratio Γ is defined by $\Gamma = s/(r_2 - r_1)$. Taking $r_2\Omega$ and $d = (r_2 - r_1)$ as characteristic velocity and length scales, we define the Reynolds number Re as $Re = r_2\Omega d/\nu$, where ν is the kinematic viscosity of the fluid. Various flow patterns appear depending on the set of parameter (Γ, Re). There is another parameter $\eta = r_1/r_2$, but the flow is not affected significantly by the value of η so that $\eta = 0.5$ is assumed throughout this paper except for comparison with experimental results.

We assume incompressible flow with the axisymmetry. Then, the velocity $\boldsymbol{u} = (u, v, w)$ in cylindrical coordinates is written in terms of Stokes' stream function ψ and a function ϕ in nondimensional form as $u = \dfrac{1}{r_\beta}\dfrac{\partial \psi}{\partial z}$, $w = -\dfrac{1}{r_\beta}\dfrac{\partial \psi}{\partial r}$ and $v = \dfrac{\phi}{r_\beta}$ where $r_\beta = r + r_1/d$. The governing equations of the flow in a frame of reference rotating with angular velocity Ω,

the continuity and Navier Stokes equations, are written in nondimensional form as

$$\frac{\partial \omega}{\partial t} - \frac{\omega}{r_\beta^2}\frac{\partial \psi}{\partial z} - \frac{1}{r_\beta}J(\psi,\omega) - \frac{2}{r_\beta^3}\phi\frac{\partial \phi}{\partial z} = \frac{1}{Re}D^2\omega - \frac{\omega}{r_\beta^2}, \quad \omega = \frac{1}{r_\beta}D^2\psi, \tag{1}$$

$$\frac{\partial \phi}{\partial t} - \frac{1}{r_\beta}J(\psi,\phi) = \frac{1}{Re}D^2\phi - 2(1-\eta)\frac{\partial \psi}{\partial z}, \tag{2}$$

where $D^2 = \dfrac{\partial^2}{\partial r^2} - \dfrac{1}{r_\beta}\dfrac{\partial}{\partial r} + \dfrac{\partial^2}{\partial z^2}$ and $J(f,g) \equiv \dfrac{\partial(f,g)}{\partial(r,z)} = \dfrac{\partial f}{\partial r}\dfrac{\partial g}{\partial z} - \dfrac{\partial f}{\partial z}\dfrac{\partial g}{\partial r}$.

The boundary conditions for ψ and ϕ are given as $\dfrac{\partial \psi}{\partial r} = \dfrac{\partial \psi}{\partial z} = \psi = 0$, $\phi = 0$ on the inner ($r = 0$) cylinder and on the two disks ($z = 0, \Gamma$), and $\dfrac{\partial \psi}{\partial r} = \dfrac{\partial \psi}{\partial z} = \psi = 0$, $\phi = -(1+\beta)$ on the outer cylinder($r = 1$).

Numerical and experimental methods

We numerically solve the steady-state equations which are obtained by omitting the time-derivative terms in Eqs. (1) and (2) in order to obtain steady axisymmetric flows ($\bar{\psi}$, $\bar{\omega}$, $\bar{\phi}$). The functions $\bar{\psi}$, $\bar{\omega}$ and $\bar{\phi}$ are expanded in a series of modified Chebyshev polynomials which satisfy their boundary conditions. By utilizing the collocation method, we obtain a set of algebraic equations for the expansion coefficients, which is solved by Newton-Raphson's method.

The linear stability of the steady axisymmetric flow is analyzed by adding disturbances ($\hat{\psi}$, $\hat{\omega}$, $\hat{\phi}$) to the steady-state solutions ($\bar{\psi}$, $\bar{\omega}$, $\bar{\phi}$). Substituting $\psi = \bar{\psi} + \hat{\psi}$, $\omega = \bar{\omega} + \hat{\omega}$ and $\phi = \bar{\phi} + \hat{\phi}$ into Eqs. (1) and (2), assuming the time dependence of the disturbances as $\hat{\psi} = \tilde{\psi}e^{\lambda t}$, $\hat{\omega} = \tilde{\omega}e^{\lambda t}$, $\hat{\phi} = \tilde{\phi}e^{\lambda t}$ and neglecting the nonlinear terms with respect to the disturbances, we obatain a set of linear disturbance equations for ($\tilde{\psi}$, $\tilde{\omega}$, $\tilde{\phi}$), which is solved in a similar way to the numerical calculations of the steady-state solution.

We perform numerical simulations to obtain time-periodic flows, where we use finite difference approximations, Euler's method for the time derivatives and a fourth-order difference approximation for spatial derivatives. The Poisson equation is solved by the S.O.R. iterative method.

We use a visualization method in experiments. Two rotational disks and the outer cylinder of radius 200 mm are made of transparent acrylic resin for visualization, while the inner cylinder of radius 50 mm made of vinyl ($\eta = 0.25$). The gap between the two disks is varied in the range of 30 mm - 90 mm. Air is used for the working fluid and the flow field is visualized by smoke of incense.

Numerical and experimental results

The flow is symmetric with respect to the inter-disk midplane at small Reynolds numbers. A typical example of symmetric flow patterns in the meridian section is shown in

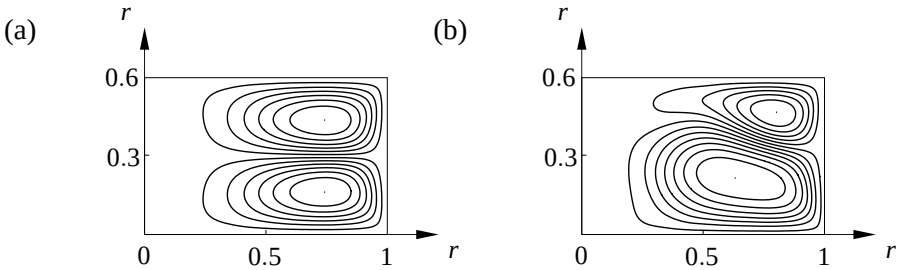

Figure 2: Flow patterns in the meridian section. $\Gamma = 0.6$, $\eta = 0.5$. (a) $Re = 950$, (b) $Re = 1200$.

Figure 2 (a) for $Re = 950$ and $\Gamma = 0.6$, in which we observe two large vortices having the same extent and opposite sense with each other. The symmetry is broken due to an instability at large Reynolds numbers. An example of such an asymmetric flow pattern is depicted in Figure 2 (b) for $Re = 1200$, where one large vortex occupies major part of the meridian section than the small one.

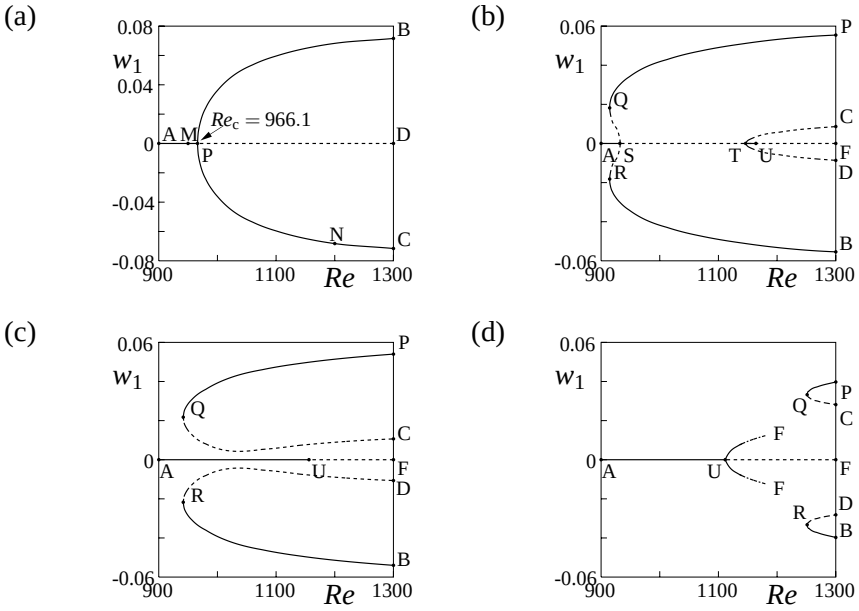

Figure 3: Bifurcation diagrams. $\eta = 0.5$. w_1: axial velocity at the point (r,z)=$(0.8, 0.5)$. Solid line: stable steady-state solution. Dashed line: unstable steady-state solution. U: Hopf bifurcation point. (a) $\Gamma = 0.60$, (b) $\Gamma = 0.69$, (c) $\Gamma = 0.694$, (d) $\Gamma = 0.720$.

In order to analyze the bifurcation structure of the flow, we choose the axial velocity w_1 at a point (r,z)=$(4/5, \Gamma/2)$ (P_1 in Figure 1) as a characteristic quantity which manifests the magnitude of asymmetry in the flow field. The bifurcation diagram is shown in Figure 3 (a) for $\Gamma = 0.6$, where solid and dashed lines indicate stable and unstable steady-state so-

lutions (steady flows), respectively. There is only one stable symmetric solution for small Reynolds number smaller than the critical value $Re_c = 966.1$, at which the symmetric solution becomes unstable and two stable asymmetric solutions appear due to a supercritical pitchfork bifurcation.

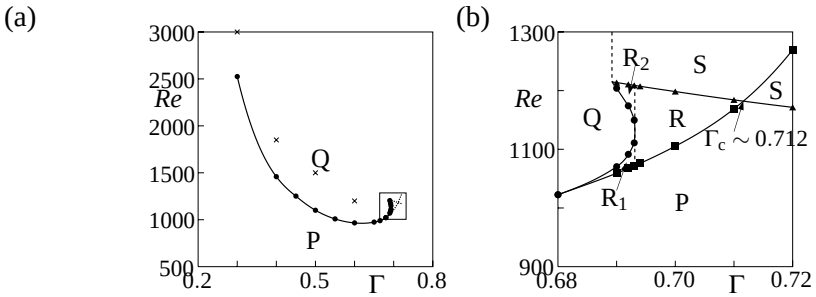

Figure 4: Transition diagram. $\eta = 0.5$. Filled circle: pitchfork bifurcation point (present result), Cross: pitchfork bifurcation point (Randriamampianina *et al.* (2001)), Filled triangle: Hopf bifurcation point, Filled square: saddle-node bifurcation point. Region P: steady symmetric flow. Region Q: steady asymmetric flow. Region R: stable steady symmetric and asymmetric flows. Region S: oscillatory flow. (a) Whole diagram, (b) Enlargement.

The bifurcation structure is almost independent of Γ in the range of $0.3 \lesssim \Gamma \lesssim 0.68$. However, as the gap ratio Γ increases up to about 0.688, the bifurcation structure changes from supercritical to subcritical and the flow becomes unstable not only to stationary disturbances but also to oscillatory ones. We show bifurcation diagrams for $\Gamma = 0.69$, 0.694 and 0.720 in Figures 3 (b), (c), (d), respectively. In Figure 3 (b), S and T indicate pitchfork bifurcation points and the point U is a Hopf bifurcation point. The critical value indicated by S becomes larger while the one by T becomes smaller as Γ increases. After getting together, the two bifurcation points disappear to yield two saddle node branches BQD and CRE, while the point U (Hopf bifurcation point) remains almost unmoved. The branch EUF indicates oscillatory flows in Figure 3 (d).

We evaluated the critical Reynolds numbers for the pitchfork and Hopf bifurcations in the range of $0.3 \lesssim \Gamma \lesssim 0.72$ and obtained a transition diagram as summarized in Figure 4 (a). In this diagram, the flow is always steady and symmetric with respect to the inter-disk midplane in region P, whereas in region Q the steady symmetric flow is unstable and two steady asymmetric flows are stable. Figure 4 (b) is an enlargement of Figure 4 (a). It is seen in this figure that the critical Reynolds number for the Hopf bifurcation becomes smaller than that for the saddle node bifurcation for $\Gamma > \Gamma_c = 0.712$. In region R, not only two steady asymmetric flows but also the symmetric flow is stable, and oscillatory flow is possible in region S.

Discussion

Researches on the condition and the mechanism for appearances of flow with a polygonal shape in the radial-tangential plane are important and interesting, which are in progress in our laboratory and will be presented at the symposium in ICCES'04.

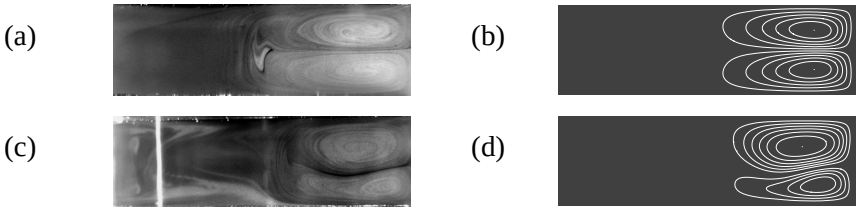

Figure 5: Flow pattern in the meridian plane. $\Gamma = 0.3$, $\eta = 0.25$. (a), (c) Experiment. (b), (d) Numerical calculation. (a) $Re = 1600$, (b) $Re = 1600$, (c) $Re = 2200$, (d) $Re = 2200$.

Reference

1. Lennemann, E. (1974): "Aerodynamic aspects of disk files," *IBM J. Res. Develop.*, Vol. 18, pp. 480-488.
2. Abrahamson, S. D., Eaton, J. K. and Koga, D. J. (1989): "The flow between shrouded corotating disks," *Phys. Fluids. A*, Vol. 1, pp. 241-251.
3. Tavener, S. J., Mullin, T. and Cliffe, K. A. (1991): "Novel bifurcation phenomena in a rotating annulus," *J. Fluid Mech.*, Vol. 229, pp. 483-497.
4. Herrero, J. and Giralt, F. (1999): "Influence of the geometry on the sturcture of the flow between a pair of corotating disks," *Phys. Fluids*, Vol. 11, pp. 88-96.
5. Randriamampianina, A., Schiestel, R. and Wilson, J. (2001): "Spatio-temporal behaviour in an enclosed corotating disk pair," *J. Fluid Mech.*, Vol. 434, pp. 39-64.